Controlled Growth and Field-Emission Properties of Cobalt Oxide Nanowalls**

By *Ting Yu*, *Yanwu Zhu*, *Xiaojing Xu*, *Zexiang Shen*, *Ping Chen*, *Chwee-Teck Lim*, *John Thiam-Leong Thong*, and *Chorng-Haur Sow**

Nanoscale materials, the basis of nanoscience and nanotechnology, have attracted a great deal of interest from researchers. Due to their large surface areas that can be exposed to gaseous environments, two-dimensional (2D) nanostructures such as nanowalls,[1] nanosheets,[2] and nanojunctions or networks[3] form an important category of nanostructured materials with great potential as important components for nanoscale devices with various interesting functions. Thus, in the past decade, many techniques have been developed for the synthesis of such nanostructured materials. For example, Lieber et al. developed the method of laser-assisted vapor–liquid–solid (VLS) growth;[4,5] the oxide-assisted growth technique was systematically studied by Lee et al.;[6] and semiconducting oxide nanobelts were fabricated by evaporating the appropriate commercial metal oxide powder.[7] More recently, metal oxide nanowires of low-melting-point metals were successfully synthesized by directly heating metal powder in a tube furnace.[8]

Cobalt oxide-based materials have many applications, such as in solid-state sensors,[9] heterogeneous catalysts,[10] electrochromic devices,[11] and as absorbers of solar energy.[12] Furthermore, Co_3O_4 nanoparticles show some interesting magnetic, optical, and transport properties.[13–15] A few methods of fabricating Co_3O_4 nanotubes and nanofibers have been reported.[16,17] However, to the best of our knowledge, there has been no report on the preparation of Co_3O_4 2D nanostructures. In this paper, we report the growth of freestanding, vertically oriented Co_3O_4 nanowalls by a surprisingly simple method: directly heating Co foil on a hot plate in ambient conditions. The dimensions, such as thickness and length, of the nanowalls were controlled by the growth temperature and duration. The field-emission properties of Co_3O_4 nanowalls were also investigated for the first time.

Figure 1a shows the scanning electron microscopy (SEM) image of the Co foil heated at 350 °C for 12 h. It reveals a surface covered with a large quantity of nanowall-like morphologies, with most of them perpendicular to the substrate. The
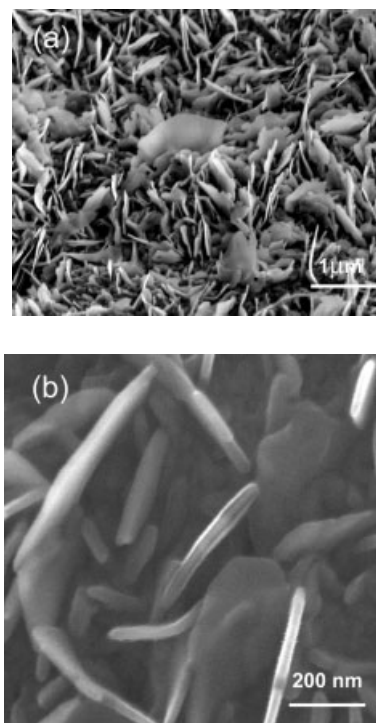

Figure 1. a) 20°-tilted SEM image of the top surface of the Co foil heated at 350 °C for 12 h. b) High-magnification image of the surface of the heated Co foil.

edges of the nanowalls are irregular and the sides of some of the nanowalls are not smooth. The high magnification image (Fig. 1b) shows that the thickness of the nanowalls fabricated using this method was around 25 nm. In order to study the composition of the as-synthesized product, the sample shown in Figure 1 was subjected to glancing-angle X-ray diffraction (GAXRD) measurements; the XRD pattern is shown in Figure 2a. Two phases of cobalt oxide, CoO and Co_3O_4, are present and no Co pattern is observed.[18] Since the top surface contributes most significantly to the GAXRD measurements, we deduce that the top layer is predominantly cobalt oxide. To further characterize the nature of the nanowalls, we scraped the nanowalls from the sample surface onto a piece of glass slide and performed micro-Raman spectroscopy on them. Figure 2b shows the Raman spectrum obtained. There are four peaks at 483, 523, 621, and 694 cm^{-1}, which correspond, re-

[*] Prof. C.-H. Sow, Dr. T. Yu, Y. W. Zhu, Prof. Z. X. Shen, Dr. P. Chen
Department of Physics, Blk S12, Faculty of Science
National University of Singapore
2 Science Drive 3, Singapore 117542 (Singapore)
E-mail: physowch@nus.edu.sg
Prof. C.-H. Sow, Y. W. Zhu, Dr. X. J. Xu, Prof. C.-T. Lim,
Prof. J. T.-L. Thong
National University of Singapore Nanoscience and
Nanotechnology Initiative
Blk S13, 2 Science Drive 3, Singapore 117542 (Singapore)
Dr. X. J. Xu, Prof. C.-T. Lim
Department of Mechanical Engineering
National University of Singapore
Blk E3A, 9 Engineering Drive 1, Singapore 117576 (Singapore)
Prof. J. T.-L. Thong
Department of Electrical and Computer Engineering
National University of Singapore
Blk E4, 4 Engineering Drive 3, Singapore 117576 (Singapore)

DOI: 10.1002/adma.200500322 © 2005 WILEY-VCH Verlag GmbH & Co. KGaA, Weinheim
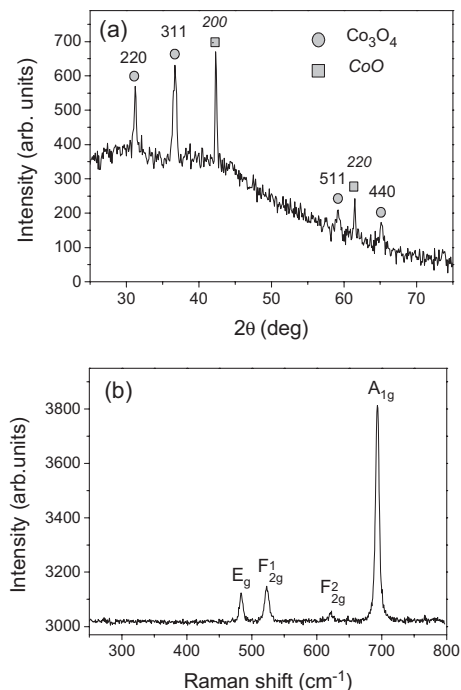
Figure 2. a) GAXRD pattern of the Co foil heated at 350 °C for 12 h. b) Micro-Raman spectrum of the nanowalls.

spectively, to the E_g, F_{2g}^1, F_{2g}^2, and A_{1g} modes of the crystalline Co_3O_4.[19] With repeated measurements of different samples, only the Co_3O_4 Raman spectrum was observed, a result that could be further strengthened by high-resolution transmission electron microscopy (HRTEM) studies of the nanowalls. In addition, it is noted that, besides the nanowalls on the top surface of the heated Co foil, there is a dense film underneath the nanowalls (Fig. 1a). Combining the XRD and Raman results, it is reasonable to attribute the dense film to CoO, as being the precursor for the growth of the Co_3O_4 nanowalls.

Figure 3a shows typical TEM images of the Co_3O_4 nanowalls lying on the carbon film of a TEM Cu grid. The nanowalls were transparent to the electron beam, which further suggests very thin walls. Figure 3b is an HRTEM image of the edge of a Co_3O_4 nanowall (highlighted by the square in Fig. 3a). The lattice fringes show a fringe spacing of 0.472 nm, corresponding to the $(\bar{1}\bar{1}1)$ plane.[18] The selected area electron diffraction (SAED) pattern of the region highlighted by the circle in Figure 3a was carried out, and the pattern is shown in Figure 3c. As indexed, the pattern of the [111] zone axes is present. Figures 3b,c clearly demonstrate that the Co_3O_4 nanowalls are single-crystalline. In this work, it is noted (see Figs. 3d–f) that some nanowalls showed complicated SAED patterns. Figure 3e shows the HRTEM image of the edge highlighted by the square in Figure 3d. The fringe spacings show good agreement with the lattice spacings of $(\bar{1}\bar{1}1)$, $(2\bar{2}0)$ and $(1\bar{3}1)$ planes, respectively. The SAED pattern of this region (highlighted by the circle in Fig. 3d) is shown in Figure 3f. Obviously, there are two patterns, with zone axes of
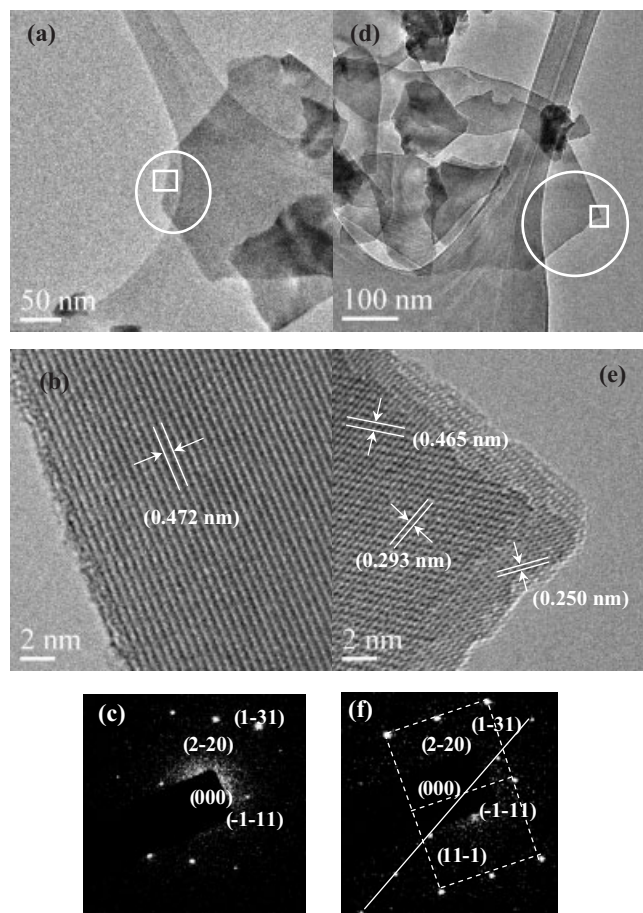
Figure 3. a) Typical TEM image of the Co_3O_4 nanowalls fabricated from Co foil after heating at 350 °C for 30 min. b) HRTEM image of the Co_3O_4 nanowall highlighted by the square in (a). c) SAED pattern of the region highlighted by the circle in (a). d) TEM, e) HRTEM, and f) SAED measurements demonstrate that some nanowalls show complicated SAED patterns. The dashed lines and solid line in (f) show the patterns of [112] and [123] zone axes, respectively.

[112] and [123]. This could be due to the overlap of the nanowalls. The detailed crystal structure of such nanowalls will be further investigated. Thus, based on the above observations, the Co_3O_4 nanowalls are single-crystalline.

To control the morphologies of the Co_3O_4 nanowalls, the effects of heating temperature and duration of heating were investigated. Co foils were heated for 1 h at different temperatures in the range 200–350 °C, or they were heated at 350 °C for different duration times, from 1 to 20 min. The dimensions of the walls, such as thickness and length, show obvious differences with the change of temperature or duration of heating. The thicknesses and lengths of the Co_3O_4 nanowalls synthesized under different conditions are plotted as a function of temperature or duration and are shown in Figure 4. A strong dependence of the dimensions on the growth conditions can be clearly seen. This suggests that the morphologies of the Co_3O_4 nanowalls could be controlled by varying the heating temperature and duration.
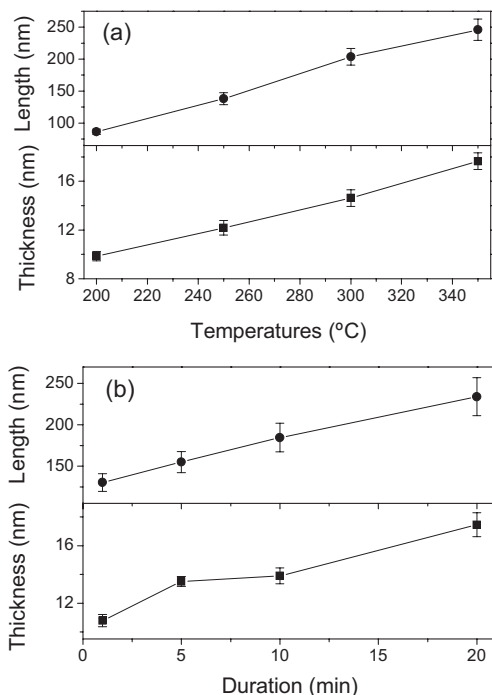
Figure 4. Plots of the dimensions (thickness and length) of the Co_3O_4 nanowalls as functions of a) heating temperature (duration was 1 h) and b) heating duration (temperature was fixed at 350 °C).

VLS[4] and vapor–solid (VS) growth[20] are two common mechanisms for producing one-dimensional (1D) and 2D nanostructures. From our SEM and TEM results, the VLS mechanism is unlikely because we do not observe terminators on the Co_3O_4 nanowalls. Considering the growth temperatures (200–350 °C), which are much lower than the boiling point of bulk Co (2927 °C),[20] VS may not be the main mechanism of the growth of the Co_3O_4 nanowalls either. To test our supposition, we flowed air at a rate of about 1.3×10^6 sccm towards the sample during the growth process. This flow rate is much larger than those normally used for the growth of nanostructures[7,8] and ensures that there is not much vapor staying above the sample surface during the heating process. The SEM image of the products under such conditions showed that the Co_3O_4 nanowalls can still be formed and the morphologies are similar to those fabricated without air flow. This suggests that vapor does not play a significant role during the growth of Co_3O_4 nanowalls. Based on these observations, we propose the following mechanism for the growth process: When the temperature of the hot plate reaches the surface

melting point of Co foil (which was suggested to be near 300 °C[22]) or even when the temperature may be high enough to melt a CoO thin layer, the surface starts to melt and forms a liquid media. Subsequently, oxygen in air may dissolve in the liquid Co and oxidize Co to CoO, which acts as the precursor for subsequent growth of the Co_3O_4 nanowalls. The CoO near the surface is further oxidized to Co_3O_4, which would precipitate after saturation in liquid media to begin the growth of the nanowalls. The growth could continue until cooling, when the liquid condenses into the solid state. Thus, the mechanism corresponding to the growth of Co_3O_4 nanowalls may belong to some kind of solid–liquid–solid (SLS) method.[23]

Since the Co_3O_4 nanowalls are vertically aligned with very rough edges (see Fig. 1), they are potential candidates for field emission (FE) studies. In this work, FE properties of the Co_3O_4 nanowalls were investigated for the first time. The details of the experimental setup and method have been described elsewhere.[24] Briefly, measurements of the FE properties of the Co_3O_4 nanowalls were carried out by using a two-parallel-plate configuration with an electrode distance of 100 μm, under a pressure of about 4×10^{-7} torr (1 torr ≈ 133 Pa). An indium tin oxide (ITO) glass covered with a layer of phosphor was employed as the anode in order to show fluorescent images simultaneously. Figure 5 shows a typical current density–electric-field (J–E) curve of the Co_3O_4 nanowalls synthesized at 350 °C for 5 h, from which we can see that the turn-on field of such Co_3O_4 nanowalls was about 6 V μm^{-1} and the maximal current density reached about 25 μA cm^{-2} (under a field of 11 V μm^{-1}). Here, the turn-on field was defined as the field at which a current density of 0.1 μA cm^{-2} was reached. Repeated measure-
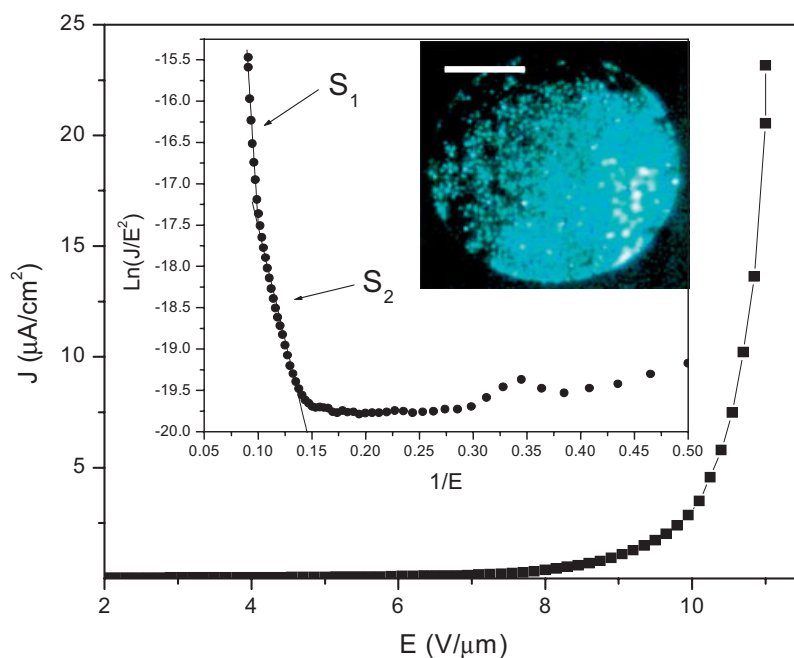
Figure 5. Typical FE J–E curve of the Co_3O_4 nanowalls. The inset depicts the Fowler–Nordheim (FN) plot, which shows a linear dependence, and a uniform FE fluorescence image with the diameter of emission area of about 2.8 mm under a field of 11 V μm^{-1}. The scale bar is 1 mm.

ment of different samples showed that the turn-on field of the Co_3O_4 nanowalls varied between 5 and 7.5 V μm^{-1}. Also, up to the maximum field of our measurement system (about 11 V μm^{-1}), no evidence of FE current saturation was observed. In addition, rather uniform FE fluorescence images were recorded under a field of 11 V μm^{-1}, as demonstrated in the picture inset of Figure 5. Such FE performance of Co_3O_4 nanowalls is comparable to many other nanostructures,[25] which makes Co_3O_4 another novel candidate for future electron emitters.

The inset graph of Figure 5 shows the FN plot (i.e., a plot of the relationship between $\ln(J/E^2)$ and $1/E$) of the field emission of the Co_3O_4 nanowalls. Two linear regions at high fields are obtained, implying that a quantum-tunneling mechanism is responsible for the emission in each range.[26] According to the FN theory,[24,26] the slope of the FN plot can be expressed as

$$S = -6.44 \times 10^3 \frac{\phi^{3/2}}{\beta} \tag{1}$$

where ϕ is the work function of emitters (in eV) and β is the field enhancement factor, defined as the ratio of the local field in the vicinity of the emitter to the average field, E (in V μm^{-1}), used in our FE measurements. The values of S can be obtained by fitting the two linear regions of the FN plot for S_1 and S_2. The work function of Co_3O_4 has been previously estimated to be 4.5 eV[27–29]. Thus, using this value and the two slope values, $S_1 = -204 \pm 13$ and $S_2 = -55 \pm 2$, the average enhancement factors were obtained to be about $\beta_1 = 302 \pm 19$ and $\beta_2 = 1118 \pm 41$. Both values are comparable to those obtained from different measurements on carbon nanotubes.[30] Finally, it is worth noting that, the two-region feature of the FN plot of the Co_3O_4 nanowalls is different from that of carbon nanotubes, for which the magnitude of the slope at higher fields generally is higher due to increased space–charge effects, interactions between neighboring emitters, and so on.[31] Such different FE behavior could be caused by more complicated edge morphologies and the 2D nature of the Co_3O_4 nanowalls, which will be further studied in our future work.

In summary, we have demonstrated a simple and convenient method to fabricate vertically oriented Co_3O_4 nanowalls supported on metal substrates. Both TEM and diffraction investigations indicate the single-crystalline property of such nanowalls. The morphologies of the Co_3O_4 nanowalls can be controlled by varying the growth temperature and duration. Our preliminary study implies the possible dominant growth mechanism could be SLS. Also, the Co_3O_4 nanowalls show promising FE performance with a reasonably uniform FE image. The turn-on fields and enhancement factors are comparable to those of many other nanomaterials. This suggests that the Co_3O_4 nanowalls or other morphologies of Co_3O_4 nanostructures could be a potentially useful electron field emitter. In addition, the properties, such as large surface area, good vertical alignment, and catalyst-free synthesis, suggest that Co_3O_4 nanowalls may have wide potential applications not only in the research laboratory, but also in industry.

Experimental

The synthesis process of Co_3O_4 nanowalls is similar to our previous work on the growth of copper oxide (CuO) nanowires on Cu foil [24,32]. We heated, polished, and cleaned Co foil (Aldrich Chem. Co., 0.1 mm thick, 99.95 %) on a hot plate in ambient conditions. In this work, the growth temperature was set within the range of 200–350 °C and the heating duration was varied from 1 min to 12 h. Typically, the heating caused the shiny surface of metallic foils to become dull and darkened. Different from the growth of CuO nanowires, where the CuO film tended to crack during cooling of samples [20,24,32], the darkened surface layer remained tightly connected with the Co substrate, which made it very convenient to directly investigate the electrical properties of the as-grown samples. The morphologies and crystalline structures of the as-grown surface layer were studied by scanning electron microscopy (SEM, JEOL JSM-6400F) and transmission electron microscopy (TEM, JEOL JEM-2010F, 200 kV), respectively. Glancing angle X-ray diffraction (GAXRD, Bruker Analytical X-Ray Systems, Cu $K\alpha$ radiation, $\lambda = 1.5406$ Å), and micro-Raman spectroscopy (ISA T64000 Triple Grating System, Ar Laser, $\lambda = 514.5$ nm) were used to analyze the structural phase and composition of the resultant surface layer.

[1] Y. H. Wu, P. W. Qiao, T. C. Chong, Z. X. Shen, *Adv. Mater.* **2002**, *14*, 64.

[2] H. Zhang, K. P. Loh, C. H. Sow, H. Gu, X. D. Su, C. Huang, Z. K. Chen, *Langmuir* **2004**, *20*, 6914.

[3] Z. L. Wang, Z. W. Pan, *Adv. Mater.* **2002**, *14*, 1029.

[4] A. M. Morales, C. M. Lieber, *Science* **1998**, *279*, 208.

[5] X. F. Duan, C. M. Lieber, *J. Am. Chem. Soc.* **2000**, *122*, 188.

[6] R. Q. Zhang, Y. Lifshitz, S. T. Lee, *Adv. Mater.* **2003**, *15*, 635.

[7] Z. W. Pan, Z. R. Dai, Z. L. Wang, *Science* **2001**, *291*, 1947.

[8] H. Y. Dang, J. Wang, S. S. Fan, *Nanotechnology* **2003**, *14*, 738.

[9] M. Ando, T. Kobayashi, S. Lijima, M. Haruta, *J. Mater. Chem.* **1997**, *7*, 1779.

[10] S. Weichel, P. J. Moller, *Surf. Sci.* **1998**, *399*, 219.

[11] L. D. Burke, M. E. Lyons, O. J. Murphy, *J. Electroanal. Chem.* **1982**, *132*, 247.

[12] K. Ramachandram, C. O. Oriakhi, M. M. Lemer, V. R. Koch, *Mater. Res. Bull.* **1996**, *31*, 767.

[13] S. Takada, M. Fujii, S. Kohiki, T. Babasaki, H. Deguchi, M. Mitome, M. Oku, *Nano Lett.* **2001**, *1*, 379.

[14] H. Yamamoto, S. Tanaka, T. Naito, K. Hirao, *Appl. Phys. Lett.* **2002**, *81*, 999.

[15] J. Tejada, X. X. Zhang, E. del Barco, E. J. M. Hernandez, E. M. Chudnovsky, *Phys. Rev. Lett.* **1997**, *79*, 1754.

[16] T. Li, S. G. Yang, L. S. Huang, B. X. Gu, Y. W. Du, *Nanotechnology* **2004**, *15*, 1479.

[17] H. Y. Guan, C. L. Shao, S. B. Wen, B. Chen, J. Gong, X. H. Yang, *Mater. Chem. Phys.* **2003**, *82*, 1002.

[18] Joint Committee on Powder Diffraction Standards. Diffraction Data File, No. 43-1004. (CoO); 43-1003 (Co_3O_4); 15-0806 (Co), International Centre for Diffraction Data.

[19] V. G. Hadjiev, M. N. Iliev, I. V. Vergilov, *J. Phys. C: Solid State Phys.* **1998**, *21*, L199.

[20] X. C. Jiang, T. Herricks, Y. N. Xia, *Nano Lett.* **2002**, *2*, 1333.

[21] http://www.webelements.com/webelements/elements/text/Co/heat.html

[22] D. L. Peng, T. J. Konno, K. Wakoh, T. Hibara, K. Sumiyama, *Eur. Phys. J. D* **2001**, *16*, 329.

[23] Y. J. Xing, Q. L. Hang, H. F. Yan, H. Y. Pan, J. Xu, D. P. Yu, Z. H. Xi, Z. Q. Xue, S. Q. Feng, *Chem. Phys. Lett.* **2001**, *345*, 29.

[24] Y. W Zhu, T. Yu, F. C. Cheong, X. J. Xu, C. T. Lim, V. B. C. Tan, J. T. L. Thong, C. H. Sow, *Nanotechnology* **2005**, *16*, 88.

[25] S. A. Johnson, M. Markwitz, H. Rudolphi, O. S. P. Baumann, K. B. K. Teo, W. I. Milne, *Appl. Phys. Lett.* **2004**, *85*, 3277.

[26] R. H. Fowler, L. W. Nordheim, *Proc. R. Soc. London, Ser. A* **1928**, *A119*, 173.

[27] http://environmentalchemistry.com/yogi/periodic/Co.html

[28] B. Klingenberg, F. Grellner, D. Borgmann, G. Wedler, *Surf. Sci.* **1993**, *296*, 374.

[29] M. R. Castell, S. L. Dudarev, G. A. D. Briggs, A. P. Sutton, *Phys. Rev. B* **1999**, *59*, 7342.

[30] S. Hofmann, C. Ducati, B. Kleinsorge, J. Robertson, *Appl. Phys. Lett.* **2003**, *83*, 4661.

[31] P. G. Collins, A. Zettl, *Phys. Rev. B* **1997**, *55*, 9391.

[32] T. Yu, X. Zhao, Z. X. Shen, Y. H. Wu, W. H. Su, *J. Cryst. Growth* **2004**, *268*, 590.

Achieving High Strength and High Ductility in Precipitation-Hardened Alloys**

By *Zenji Horita*, *Kunihiro Ohashi*, *Takeshi Fujita*, *Kenji Kaneko*, and *Terence G. Langdon**

It is now well established that the processing of metals through the application of severe plastic deformation (SPD) leads to significant grain refinement to the submicrometer or nanometer level:[1] an example of SPD is the procedure of equal-channel angular pressing (ECAP). Although the ultrafine-grained materials produced by SPD have high strength, in accordance with the Hall–Petch relationship, and a potential for use in a wide range of structural applications, their utility is generally restricted because they exhibit only limited ductility.[2] This problem may be overcome at cryogenic temperatures by combining ECAP with subsequent cold-rolling (CR),[3] but this approach is not effective at ambient temperatures because of the advent of grain growth. Alternatively, high strength and high ductility have been achieved in pure copper by developing a special thermomechanical treatment

to produce a bimodal grain size.[4] However, the viability of this procedure is limited because new thermomechanical treatments must be developed for each selected alloy. We now report a technique for producing high strength and high ductility in precipitation-hardened alloys at ambient temperatures, based on the introduction of intermediate metastable phases into ultrafine-grained microstructures.

The experiments were conducted using an aluminum–silver alloy containing 10.8 wt.-% Ag; this alloy was selected because it is well established that Al–Ag alloys are capable of exhibiting significant hardening through aging treatments due to the formation of the metastable γ'-phase.[5] Full details of the material preparation and the experimental procedures are given in the Experimental section. Briefly, the material was prepared in a solution-treated condition with a grain size of ∼ 480 μm, and some of the solution-treated samples were further processed either by CR, to give an elongated grain structure, or by ECAP, to give an equiaxed microstructure with an average grain size of ∼ 500 nm. Ageing treatments were conducted after solution treatment (ST), after ST and subsequent CR, and after ST and subsequent ECAP.

Figure 1 shows the Vickers microhardness, HV, as a function of the aging time for billets in the solution-treated condition, and after ST followed by CR or ECAP. These results reveal several significant trends. Firstly, the microhardness is initially
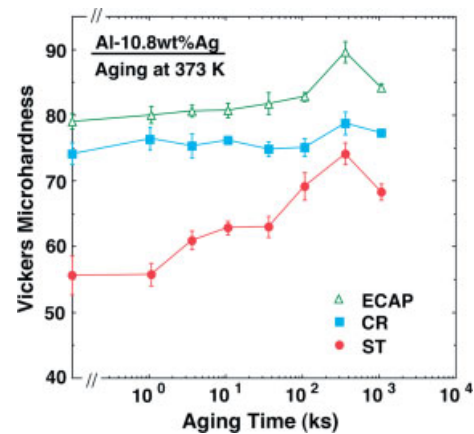

Figure 1. Variation of Vickers microhardness with aging time at 373 K for samples after ST, CR, and ECAP.

relatively low in the solution-treated condition, $HV \approx 56 \pm 3$, but it increases with aging time and reaches a peak value of $HV \approx 74 \pm 2$ after aging for 100 h (3.6×10^5 s). Secondly, the values of HV are higher after CR but there is only a minor increase with aging time. Thirdly, the highest values of HV are recorded after ECAP, with a value of $HV \approx 79 \pm 1$ in the absence of aging and a peak value of $HV \approx 90 \pm 2$ after aging for 100 h. Under all three conditions, the values of HV decrease at aging times longer than 100 h. The high values of HV attained after ECAP are due to the high strain imposed during processing and the consequent refinement of the microstructure into an array of ultrafine grains with boundaries

[*] Prof. T. G. Langdon
Department of Aerospace & Mechanical Engineering
Department of Materials Science
University of Southern California
Los Angeles, CA 90089-1453 (USA)
E-mail: Langdon@usc.edu
Prof. Z. Horita, K. Ohashi, Prof. K. Kaneko
Department of Materials Science and Engineering
Faculty of Engineering, Kyushu University
Fukuoka 812-8581 (Japan)
Dr. T. Fujita
Center for Solid State Sciences, Arizona State University
Tempe, AZ 85287-1704 (USA)

DOI: 10.1002/adma.200500069